World Academy of Science, Engineering and Technology
International Journal of Physical and Mathematical Sciences
Vol:4, No:1, 2010

Migration of a Drop in Simple Shear Flow at Finite Reynolds Numbers: Size and Viscosity Ratio Effects

M. Bayareh, S. Mortazavi

***Abstract*—**The migration of a deformable drop in simple shear flow at finite Reynolds numbers is investigated numerically by solving the full Navier-Stokes equations using a finite difference/front tracking method. The objectives of this study are to examine the effectiveness of the present approach to predict the migration of a drop in a shear flow and to investigate the behavior of the drop migration with different drop sizes and non-unity viscosity ratios. It is shown that the drop deformation depends strongly on the capillary number, so that; the proper non-dimensional number for the interfacial tension is the capillary number. The rate of migration increased with increasing the drop radius. In other words, the required time for drop migration to the centreline decreases. As the viscosity ratio increases, the drop rotates more slowly and the lubrication force becomes stronger. The increased lubrication force makes it easier for the drop to migrate to the centre of the channel. The migration velocity of the drop vanishes as the drop reaches the centreline under viscosity ratio of one and non-unity viscosity ratios. To validate the present calculations, some typical results are compared with available experimental and theoretical data.

***Keywords*—**drop migration, shear flow, front-tracking method, finite difference method.

I. Introduction

THE motion of drops and particles in a fluid medium in channel and pipe flows is of fundamental importance in the processing of materials in the reduced gravity environment and in a wide variety of technologically important processes. Some works have been performed to investigate the motion of drops and particles in the fluid medium at the Reynolds number of either zero or O(1). Experimentally, the phenomena have been measured (initially by Taylor 1934) [1] even though the shear flows considered have been restricted in most investigations to simple shear in a Couette device. Karnis and Mason (1967) [2] reported that neutrally buoyant particles stabilized midway between the centreline and the wall in a channel, closer to the wall for larger flow rates and closer to the centre for larger particles. Halow & Wills (1970) [3] did experiments in a concentric cylindrical Couette device. They observed that when the inner cylinder rotates, a particle migrates from any initial position to equilibrium at a small distance inside the centreline of the gap. Rallison (1980) [4] has studied the time-dependent deformation and burst of a viscous drop in an arbitrary shear flow at zero Reynolds number. He presented a numerical scheme to track the two-dimensional drop shape in time. Magna & Stone (1993) [5] reported the time-dependent interactions between two buoyancy-driven deformable drops in a low Reynolds number flow. They introduced three modes for film drainage between the drops: rapid drainage, uniform drainage and dimple formation. As the separation distance between the two drops decreases, the mode of film drainage may change from rapid drainage to uniform drainage and eventually a dimple may form. Zhou & Pozrikidis (1993) [6] studied the flow of periodic suspension of two-dimensional viscous drops in a closed channel that was bounded by two parallel plane walls. They found that there exists a critical capillary number below which the suspensions exhibit stable periodic motion, and above which the drops elongate and tend to coalesce, altering the topology of the initial configuration. They studied the effects of capillary number, viscosity ratio, volume fraction of dispersed phase, lattice geometry, and instantaneous drop shape, on the effective stress tensor of the suspension. Feng *et al.* (1994) [7] reported the results of a two-dimensional finite element simulation of the motion of a circular particle in a Couette & Poiseuille flow. They showed that a neutrally buoyant particle migrates to the centerline in a Couette flow and the stagnation pressure on the particle surface is particularly important in determining the direction of migration. Li *et al*. (1995) [8] studied the motion of two-dimensional, doubly periodic, dilute and concentrated emulsions of liquid drops with constant surface tension in a simple shear flow. Their numerical method is based on a boundary integral formulation. They showed that the shearing flow is able to stabilize a concentrated emulsion against the tendency of the drops to become circular and coalesce, thereby allowing for periodic evolution even when the volume fraction of suspended phase might play a role similar to that of the foam. Loewenberg & Hinch (1996) [9] did a three-dimensional simulation of a concentrated emulsion in shear flow, for zero-Reynolds-number and finite-capillary-numbers. Results were obtained for dispersed-phase volume fractions up to 30% and dispersed to continues-phase viscosity ratios in the range of 0 to 5. They reported the viscosity of an emulsion is only moderately increasing function of the dispersed-phase volume fraction, in contrast to suspensions of rigid particles or

M. Bayareh, Islamic Azad University (IAU), Branch of Lamerd, Lamerd, Fars, Iran; (email: mbayareh@ me.iut.ac.ir).

S. Mortazavi, Isfahan University of Technology (IUT), 84156-83111, Daneshjoo square, Isfahan, Iran; (e-mail: saeedm@cc.iut.ac.ir).

undeformed drops. Esmaeeli & Tryggvason (1998) [10] simulated the motion of two-and three-dimensional buoyant bubbles. They compared a finite Reynolds number two-dimensional simulation with sixteen bubbles and a Stokes flow simulation and reported that the finite Reynolds number array break up much faster. Their simulations showed a slight increase in the average rise velocity compared to a regular array. Mortazavi & Tryggvasson (1999) [11] studied the motion of a drop in Poiseuille flow. They simulated the motion of many drops at finite Reynolds numbers. Esmaeeli & Tryggvason (1999) [12] simulated the motion of two-and three-dimensional finite Reynolds number buoyant bubbles. They showed that the rise Reynolds number is nearly independent of the number of bubbles, the velocity fluctuations in the liquid (the Reynolds stresses) increase with the size of the system. Balabel *et al.* (2002) [13] introduced a numerical model based on the level set method for computing unsteady droplet internal flows. They presented this model for linear droplet oscillation processes. Crowdy (2003) [14] studied the problem of a two-dimensional inviscid compressible bubble evolving in Stokes flow. They reported that if the ambient pressure is small enough, bubbles can expand significantly. In addition, they showed that a bubble evolving adiabatically is less likely to expand than an isothermal bubble. Yoon *et al.* (2005) [15] investigated experimentally the effect of the dispersed to continues-phase viscosity ratio on the flow-induced coalescence of two equal-sized drops with clean interfaces. Their study showed that when the viscosity ratio is greater than $O(0.1)$, the critical capillary number decreases with increasing offset only for the smallest offsets, but increases with increasing offset until a critical offset is reached above which coalescence in not observed. Norman *et al.* (2005) [16] studied the neutrally buoyant particles in a low-Reynolds-number pressure-driven flow. They showed that when the particle density differs from that of the suspending fluid, buoyancy forces also affect particle migration. They reported that suspension flows become fully developed earlier than that observed for neutrally buoyant particles. Yang *et al.* (2005) [17] simulated the migration of a sphere in tube flow. They presented a formula for the lift force. Their formula predicted the change of sign of the lift force. They compared their correlation formula with analytical lift formula and showed that the equilibrium position moves toward the wall as the Reynolds number increases at a fixed drop radius and it moves towards the centreline as the radius of drop increases at a fixed Reynolds number.

Sibillo *et al*. (2007) [18] investigated the deformation and breakup of a drop in an immiscible equiviscous liquid undergoing unbounded shear flow. They showed that wall effects can be exploited to obtain nearly monodisperse emulsions in microconfined shear flow. Zhao (2007) [19] investigated the drop break up in dilute Newtonian emulsions in simple shear flow by using high-speed microscopy over a wide range of viscosity ratio, focusing on high capillary number. He showed that the final drop size distribution intimately links to the drop break up mechanism, which depends on viscosity ratio and capillary number.

Numerical and experimental results have been obtained for the evolution of the following quantities during migration: the particle trajectory, the slip velocity of the particles, the initial size of the particles, the migration velocity, distribution of pressure and viscous stresses on the surface of the particles, and the deformation parameter.

Theoretical analysis of the lateral migration of deformable drops in a channel flow was restricted to the two-dimensional Stokes and potential flows. The objectives of this study are to examine the effectiveness of the present approach to predict the migration of a drop in a shear flow and to investigate the behavior of the drop migration with different drop sizes and non-unity viscosity ratios at finite Reynolds numbers by adding the advection terms to the governing equations.

Section 2 contains the formulation, and a short description of the numerical method.

II. FORMULATION AND NUMERICAL METHOD

A. Governing equations

The governing equations for the motion of unsteady, viscous, incompressible, immiscible two- fluid systems are the Navier-Stokes equations in conservative form:

$$\partial \rho u / \partial t + \nabla . \rho u u = -\nabla P + \nabla . \mu (\nabla u + \nabla u^T) + \sigma \int \kappa n \delta^{\beta} (x - X) d_S \quad (1)$$

Here u is the fluid velocity, p is the pressure, ρ is the fluid density, μ is the fluid viscosity, and σ is the surface tension coefficient. δ^{β} is a two- or three-dimensional delta function. The dimension is denoted by $\beta = 2$ or 3. κ is the curvature for two-dimensional flows and twice the mean curvature for three-dimensional flows. n is a unit vector normal to the drop surface pointing outside of the drop. x is the position in Eulerian coordinate and X is the position of front in Lagrangian coordinate.

Both of fluids are taken to be incompressible, so the divergence of velocity field is zero:

$$\nabla . u = 0 \quad (2)$$

Equations of state for the density and the viscosity are:

$$D\rho / Dt = 0, \; D\mu / Dt = 0 \quad (3)$$

where, D/Dt is the material derivative and these equations state that the density and the viscosity of each fluid remain constant.

By integrating the normal component of Eq. (1) over a small volume containing the interface, most of the terms gets to zero, and in the limit of infinitesimal volume:

$$\left[-pI + \mu (\nabla u + \nabla u^T) \right] \cdot n = \sigma \kappa n \quad (4)$$

where the brackets denote the jump across the interface. This is the usual statement of continuity of stresses at a fluid boundary, showing that the normal stresses are balanced by surface tension. In the similar way, integrating the tangential components shows that the tangential stresses are continuous.

B. Numerical method

Various methods have been used to simulate the two-phase flows. These methods include: (1) capture the front directly on a regular, stationary grid. The best known examples are the marker-and-cell (MAC) method, where marker particles are used to identify each fluid, the volume-of-fluid (VOF) method, where a marker function is used, and level sets method, where the fluid interface marker is used. (2) use separate, boundary fitted grids for each phases. (3) Lagrangian methods where the grid follows the fluid. (4) front tracking, where a separate front marks the interface but a fixed grid, only modified near the front to make a grid line follow the interface, is used for the fluid within each phase. In addition to front tracking methods that are applicable to the full Navier Stokes equations, specialized boundary integral methods have been used for both potential and Stokes flows. In general, the interface representation can be explicit (moving mesh) or implicit (fixed mesh) or a combination of both. The front-tracking method is a combination of fixed and moving mesh method. Although an interface grid tracks the interface, the flow is solved on a fixed grid. The interface conditions are satisfied by smoothing the interface discontinuities and interpolating interface forces from the interface grid to the fixed grid. In this method, the governing equations are solved for whole flow field. The first is a sharp boundary between the fluids and the second is accurate computation of surface tension. Different methods have been made in overcoming these problems.

The front is resolved by discrete computational points that are moved by interpolating their velocities from the grid. These points are connected by triangular elements to form a front that is used to keep the density and viscosity stratification sharp and to calculate surface tension. At each time step information must be passed between the front and the stationary grid. This is done by a method that discussed by Unverdi & Tryggvason (1992) [20], where the density jump is distributed to the grid points next to the front and a smooth density field that changes from one density to the other over two to three grid spaces generated by the solution of a Poisson equation. While this replaces the sharp interface by a slightly smoother grid interface, numerical diffusion of the density and the viscosity fields is eliminated, since the grid field is reconstructed at each step.

The spatial differentiation is calculated by second order finite difference on a staggered Eulerian grid. An explicit second-order time integration method is used. Combining the incompressibility condition and momentum equations results in a non-separable elliptic equation for the pressure. Due to the equality in density between the drop and the ambient fluid, a quick Poisson solver (FICHPACK) solves the pressure equation.

The force due to surface tension on each element of front is

$$\delta F_\sigma = \int_{\Delta S} \sigma \kappa n \, d_S \tag{5}$$

In three-dimensional flow, the average surface curvature is

$$\kappa n = (n \times \nabla) \times n \tag{6}$$

Then, the force on each element surface is

$$\delta F_\sigma = \sigma \int_{\delta A} \kappa n d_A = \sigma \int_{\delta A} (n \times \nabla) \times n d_A = \sigma \oint_S \tau \times n d_S \tag{7}$$

The integration is over the boundary of each element representing the front. τ and n are the tangent and the normal vector to each element, respectively.

III. RESULTS

The effects of the drop size and viscosity ratio on the cross-stream migration of a drop in simple shear flow are presented. The drop diameter is D, and the height of the channel is H. The top wall is moving at velocity U in x-direction, and bottom wall is stationary. The boundary conditions are periodic in the x- and y-direction and rigid, top and bottom walls in the z-direction (Figure 1).

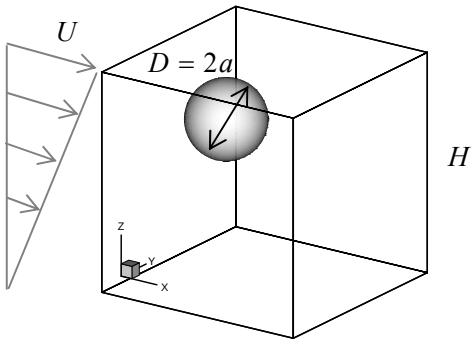

Fig. 1 Migration of a drop in simple shear flow between no-slip walls.

Numerical simulations of the migration of a drop in simple shear flow were performed over a range of values of the governing non-dimensional parameters of the flow. These parameters are: (i) the viscosity ratio $\lambda = \mu_d / \mu_\circ$, where $\mu_\circ$ and μ_d are the viscosities of ambient fluid and of the drop, respectively, (ii) The density ratio $\eta = \rho_d / \rho_\circ$, where $\rho_\circ$ and ρ_d are the densities of ambient fluid and of the drop, respectively, (iii) The Reynolds number (particle and bulk Reynolds numbers): $Re_P = \rho_\circ \dot{\gamma} a^2 / \mu_\circ$ and $Re_b = \rho_\circ \dot{\gamma} H^2 / \mu_\circ$, where $\dot{\gamma} = (u_t - u_b)/H$ is the shear rate. u_t and u_b are top and bottom wall velocities, respectively. (iv) The capillary number $Ca = \mu_\circ \dot{\gamma} a / \sigma$, where σ is the interfacial tension. The

capillary number is the ratio of viscous force to surface-tension force, (v) The Weber number $We = \rho_\circ \dot{\gamma} a^3 / \sigma$. The Weber number is the ratio of inertial force to surface-tension force. It should be pointed out that the Weber number and the capillary number are related by $We = (Re_b)(Ca)(1/\dot{\gamma})(a/H)^2$, so only one of them should be considered in the present study.

To choose a proper dimensionless parameter for the interfacial tension (i.e. either the Weber number or the capillary number), two sets of simulations were performed at constant capillary number and constant Weber number, keeping the Reynolds number constant. In other words, a set of simulation were performed with different drop sizes at a certain Reynolds number while the capillary number was constant. As a result the Weber number changed in these simulations. Another set of simulations were performed with different drop sizes at the same Reynolds number while the Weber number was constant. As a result the capillary number changed in these simulations.

The Taylor deformation, *De*, defined as (*L*-*B*)/(*L*+*B*), where *L* and *B* are, respectively, the major and minor axis of deformed drop (defined by the largest and smallest distance of the surface from the centre). Figure 2 shows the deformation of the drops as a function of dimensionless time in the two sets of simulations. Time has been normalized by the shear rate $\dot{\gamma}$ ($t^* = t \times \dot{\gamma}$). It can be seen (figure 2a) that the deformations of drops are nearly the same when the capillary number is constant. When simulations were performed at a constant Weber number (figure 2b) the drop deformation also changed as a result. Therefore, the drop deformation is a strong function of the capillary number, and in order to fix the drop deformation the capillary number should be fixed. As a result, the proper non-dimensional number for the interfacial tension is the capillary number.

So, for studying the drop size and viscosity ratio effects, the simulations were performed at fixed capillary numbers.

A. Size effects

Perturbation theories of viscous or inertial type are valid for small particle Reynolds numbers, i.e. $Re_p << \xi^2$ (Ho & Leal 1974 [21]), where $\xi = a/H$ is the geometric ratio. This condition is not satisfied in this study. In this work, results have been obtained for $Re_b = 10$ and $\xi = 0.18$, 0.2, and 0.22, so that, $Re_p = 0.324$, 0.4, and 0.484, respectively and these values are greater than $\xi^2 = 0.0324$, 0.04, and 0.0484.

It is known that a neutrally buoyant rigid particle always migrates to the centre of the channel, regardless of initial position and velocity (Feng *et al.*, 1994). They simulated the motion of solid bodies in a Newtonian fluid. Karnis and Mason (1967) considered the creeping Couette flow in a coaxial cylinder. They showed the direction of drop migration is independent of speed and direction of rotation of the cylinder walls. The results of present simulations can be compared qualitatively with the numerical results of (Feng *et al.*, 1994) and the experimental results of Karnis and Mason (1967). Figure 3 shows the lateral migration of a drop with different sizes. The lateral migration of the drop is illustrated by the dimensionless distance from the bottom of the channel. In this figure for present work: $Re_b = 10$ and $Ca = 0.2$, for results of Feng et al.: $Re_b = 40$, and for results of Karnis & Mason; dimensionless time = $t^*/7$, open triangles: $Re_b = 0.001$, $Ca = 0.65$; open circles: $Re_b = 0.0003$, $Ca = 0.185$. It can be seen that the rate of migration increases with increasing the drop radius. In other words, the required time for drop migration to the centreline decreases.

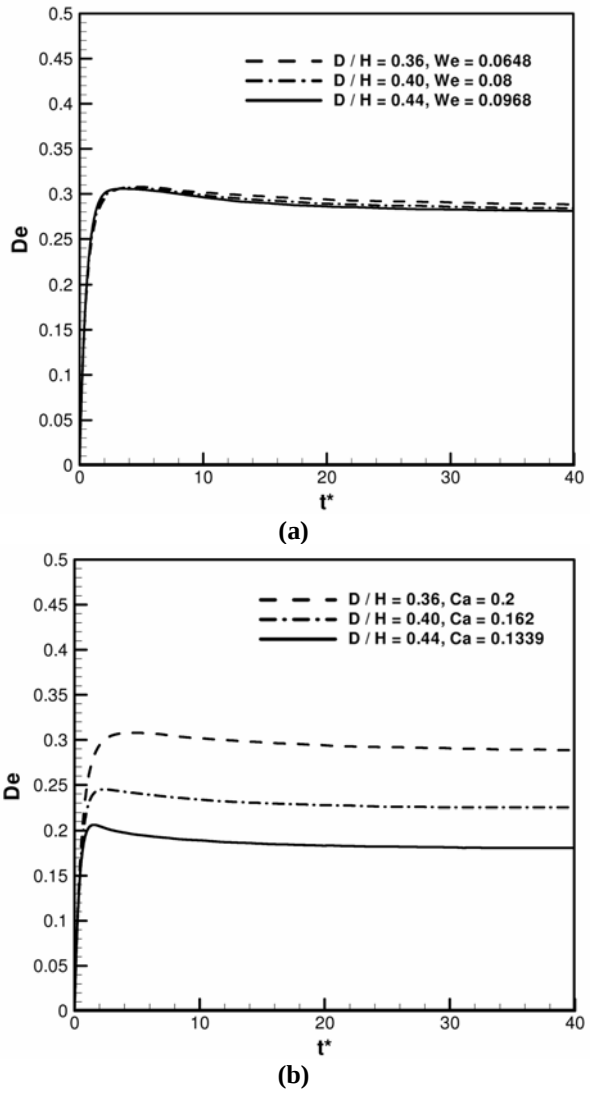

Fig. 2 drop deformation at $\lambda = \eta = 1$ and $Re_b = 10$. (a) $Ca = 0.2$, (b) $We = 0.0648$.

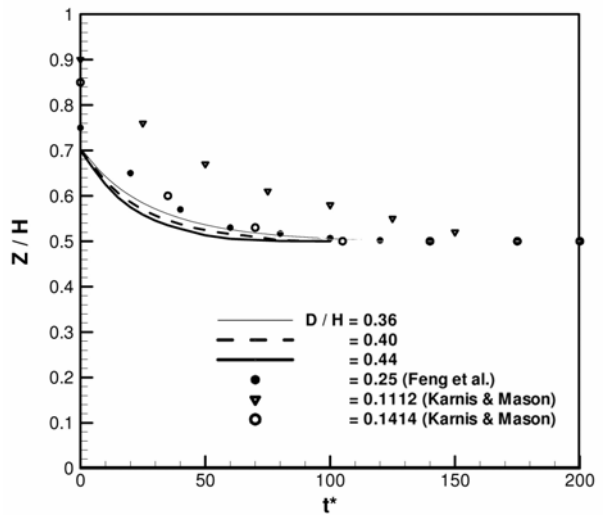

Fig. 3 Lateral migration of a drop in a simple shear flow ($\lambda = \eta = 1$).

The difference between the drop velocity and the undistributed velocity at the centre of the drop is the slip velocity δV. In figure 4 the slip velocity δV normalized by the wall velocity U is plotted. In all cases, the angular velocity rapidly relaxes from zero and the drop rotates with the local angular velocity of the flow field to within a small correction. The maximum value of the slip velocity in initial transient period is increasing with the drop radius. After the transient period, the drop is forced to lead the local undistributed velocity. Feng *et al*. (1994) obtained a similar result for a rigid sphere in a Couette flow.

The migration velocity (U_Z) of the drop along the velocity gradient direction depends on initial size at the early stage of migration (figure 5). The analytical result of Vasseur & Cox (1976) [22] for a bounded domain has also been shown for comparison. The two-dimensional results of Vasseur & Cox (1976) are for small spheres in a slow flow, and their analysis does not address transient effects. The initial position of the drop is $Z = 0.7H$. The centerline of the channel is at $Z/H = 0.5$. The sign of U_Z for result of Vasseur & Cox has been changed for comparison. In present work: $Re_b = 10$, $Ca = 0.2$; the particle Reynolds number is 0.324 for $D/H = 0.3$, is 0.40 for $D/H = 0.4$, and is 0.484 for $D/H = 0.44$.

Figure 5 shows that after the transient period, the trends are alike. Also, it can be seen that the difference between present simulations and the perturbation theory becomes larger when Re_p gets larger or the inertial effect gets stronger.

B. Effect of the viscosity ratio

The effect of viscosity ratio is described in this section at a fixed capillary number $Ca = 0.2$. Figure 6 shows the results from numerical simulations with viscosity ratios in the range $0.8 \le \lambda \le 2$ and a fixed drop radius ($a = 0.18\ H$). It can be seen that the rate of migration increases with increasing the viscosity ratio. The wall repulsion, which is a lubrication effect, is the major mechanism for drop migration (Feng ea al, 1994). In the presence case, the relative motion of the drop to the nearby wall induces this repulsion that makes the centre an equilibrium.

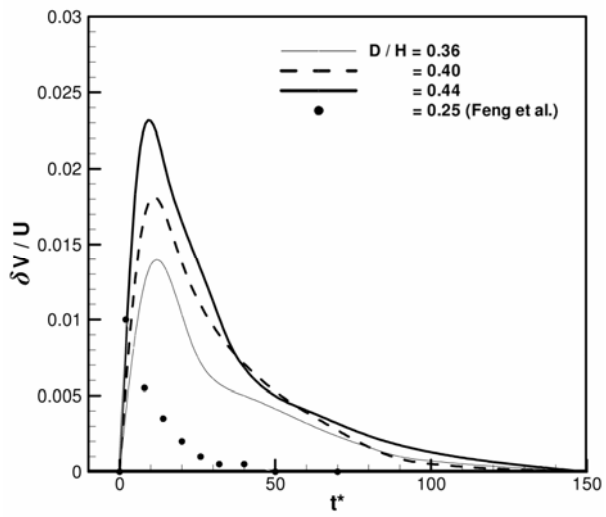

Fig. 4 Relaxation of the slip velocity δV of drops migrating in simple shear flow ($\lambda = \eta = 1$). Present work: $Re_b = 10$ and $Ca = 0.2$; Feng et al.: Rigid particle, $Re_b = 40$.

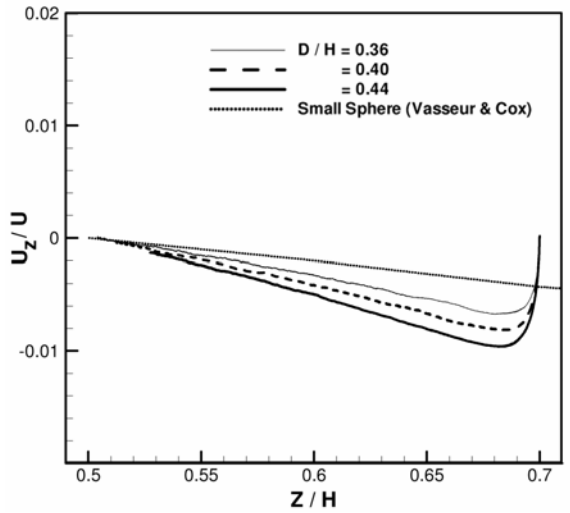

Fig. 5 Comparison of the migration velocity predicted by present simulation ($\lambda = \eta = 1$) and the theoretical result of Vasseur & Cox (1976) for small spheres.

In figure 7 the deformation parameter of the drop is plotted as a function of dimensionless time. As the viscosity ratio increases, the drop deformation slightly decreases and reaches a steady state value. As expected, the drop deformation is an decreasing function of the viscosity ratio, although at fixed capillary number, this dependency is approximately weak.

It is found that the migration velocity (U_Z) of the drop decreases smoothly as the drop reaches the equilibrium -

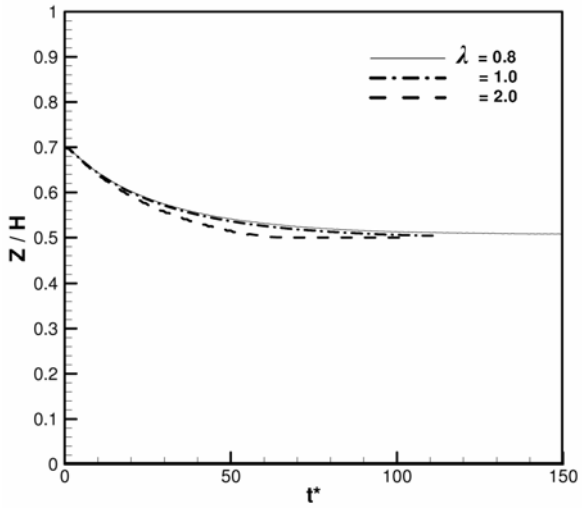

Fig. 6 Lateral migration of a drop in a simple shear flow for different λ. $\eta = 1$, $\xi = 0.18$, $Re_b = 10$, and $Ca = 0.2$.

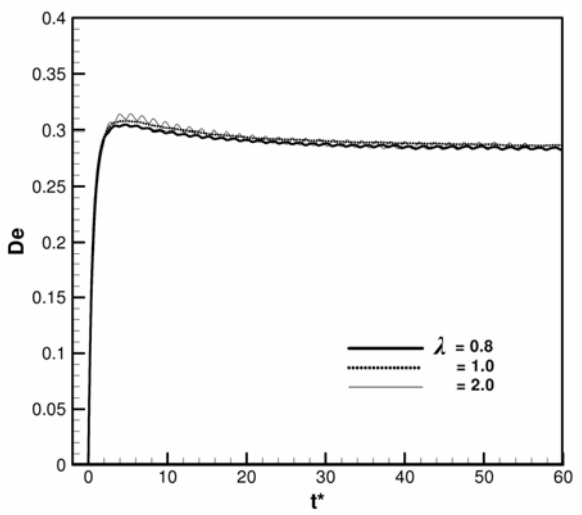

Fig. 7 drop deformation at $\eta = 1$, $\xi = 0.18$, $Re_b = 10$, and $Ca = 0.2$.

position under viscosity ratio of one and non-unity viscosity ratios. Figure 8 shows this article and confirms that the rate of migration increases with increasing the viscosity ratio. The initial position of the drop is $Z = 0.7H$. The centerline of the channel is at $Z/H = 0.5$. The sign of U_Z for result of Vasseur & Cox has been changed for comparison. In present work: $\eta = 1$, $\xi = 0.18$, $Re_b = 10$, $Ca = 0.2$.

IV. CONCLUSION

Size and viscosity ratio effects on the migration of a deformable drop in simple shear flow at finite Reynolds numbers have been studied using a finite difference/front tracking method. The results show that the drop deformation depends strongly on the capillary number.

The rate of migration increased with increasing the drop radius. So, the required time for drop migration is decreasing

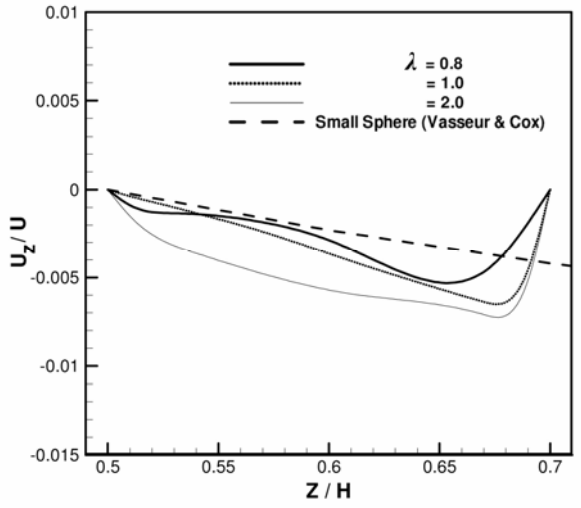

Fig. 8 Comparison of the migration velocity predicted by present simulation and the theoretical result of Vasseur & Cox (1976) for small spheres.

function of the drop radius. As the size of drop gets larger, the maximum value of the slip velocity in the initial transient period increases.

The calculations also indicate that as the viscosity ratio increases, the drop rotates more slowly and the lubrication force becomes stronger. The increased lubrication force makes it easier for the drop to migrate to the centre of the channel. As expected, the drop deformation is a decreasing function of the viscosity ratio. The migration velocity of the drop decreases smoothly as the drop reaches the equilibrium position under viscosity ratio of one and non-unity viscosity ratios.

REFERENCES

[1] Taylor, G.I., The deformation of emulsions in definable fields of flow, Proc,Ray.Soc. (London), 1934, A146, 501-523.
[2] Karnis,A. and Mason,S.G., Particle motions in sheared suspensions. XXIII. Wall migration of fluid drops, J.Colloid and Inerface. Science, 1967, 24, 164-169.
[3] Halow,J.S., and Willis,G.B., Radial migration of spherical particles in Couette system, AICHE J., 1970, 16, 281-286.
[4] Rallison, J.M., The deformation of small viscous drops and bubbles in shear flows, Annu, Rev. Fluid Mech., 1984, 16, 45-66.
[5] Magna, M. and Stone, H.A., Buoyancy-driven interactions between two deformable viscous drops, J.Fluid Mech, 1993, 256, 647-683.
[6] Zhou, H. and Pozrikidis,C., The flow of suspensions in channels: single files of drops, Phys. Fluids, 1993, A5(2), 311-324.
[7] Feng, J., Hu, H.H., and Joseph, D.D., Direct simulation of initial value problems for the motion of solid bodies in a Newtonian fluid. Part2. Couette and Poiseuille flows, J.Fluid Mech, 1994, 277, 271-301.
[8] Li, X., Zhou H. and Pozrikidis,C., A numerical study of the shearing motion of emulsions and foams, J.Fluid Mech, 1995, 286, 374-404.
[9] Loewenberg, M. and Hinch, E., Numerical simulation of a concentrated emulsion in shear flow, J.Fluid Mech., 1996, 321, 395-419.
[10] Esmaeeli, A., and Tryggvason, G., Direct numerical simulations of bubbly flows Part1. Low Reynolds number arrays, J.Fluid Mech, 1998, 377, 313-345.
[11] Mortazavi, S.S. and Tryggvasson, G., A numerical study of the motion of drop in Poiseuille flow, part1: lateral migration of one drop, J.Fluid Mech, 1999, 411, 325-350.

[12] Esmaeeli, A., and Tryggvason, G., Direct numerical simulations of bubbly flows Part2. Low Reynolds number arrays, J.Fluid Mech, 1999, 385, 325-358.
[13] Balabel A., Binninger B., Herrmann M. and Peters N., Calculation of droplet deformation by surface tension effects using the Level Set method, J. Combustion Science and Technology, 2002, 174, 257-278.
[14] [Crowdy D.G., Compressible bubbles in Stokes flow, J. Fluid Mech., 2003, 476, 345-356.
[15] Yoon Y., Borrell M., Park C.C., and Leal G., Viscosity ratio effects on the coalescence of two equal-sized drops in a two-dimensional linear flow, J. Fluid Mech., 2005, 525, 355-379.
[16] Norman, J.T., Nayak, H.V., and Bonnecaze T.B., Migration of buoyant particles in low-Reynolds-number pressure-driven flows, J. Fluid Mech., 2005, 523, 1-35.
[17] Yang B.H., Wang J., Hu H.H., Pan T.W., and Glowinski R., Migration of a sphere in tube flow, J. Fluid Mech., 2005, 540, 109-131.
[18] Sibillo, V., Pasquariello, G., Simeone, M., Cristini, V., and Guido, S., Drop deformation in micro confined shear flow, PhysRevLett, 2007, 97, pp. 2-4.
[19] Zhao, X., Drop break up in dilute Newtonian emulsions in simple shear flow: new drop break up mechanism. J. Rheology, 2007, 51, 367-192.
[20] Unverdi, S.O., and Tryggvason, G., Computations of multi-fluid flows, J. Physics, 1992, D60, 70-83.
[21] Ho, B. P., and Leal, L. G., Inertial migration of rigid spheres in two-dimensional unidirectional flows, J. Fluid Mech., 1974, 65, 365-383.
[22] Vasseur, P., and Cox, R.G., The lateral migration of a spherical particle in two-dimensional shear flow, J. Fluid Mech., 1976, 78, 385-402.
[23] Janssen, P.J.A., and Anderson, P.D., A boundary integral model for drop deformation between two parallel plates with non-unit viscosity ratio drops, J. of Computational Physics, 2008, 227, 8807-8819.